

## Simulating air distribution and comfort of three ventilation schemes

Zheng He, Xuan Gu <sup>a,\*</sup>, Xiaoyu Sun, Jianxin Teng, Binsheng Wang

College of Aerospace and Civil Engineering, Harbin Engineering University, Harbin, 150001 China

<sup>a,\*</sup>Correspondent author: guxuan@hrbeu.edu.cn

### Abstract

Excellent air distribution is an indispensable factor to acquire comfortable environment in high density occupant areas, such as subway stations. This study assesses the air distribution by adopting three different air supply schemes (mixing ventilation, stratified air ventilation and air curtain ventilation) for a subway platform. The simulation results are discussed in detail by considering air velocity, air temperature, age of air and Relative Warmth Index (RWI). It was demonstrated that air curtain ventilation presented an appropriate velocity and temperature distribution, which provides a healthy and comfortable environment. Focusing on the air curtain ventilation scheme, four cases were investigated to indicate the air velocity and temperature distribution in the occupied region. It is indicated that the highest velocities and the lowest temperatures were both achieved at the height of 0.2 m above the floor. Dimensionless velocity with different air supply velocity was proposed in this paper. This research is applicable for air curtain ventilation design appropriate for subway platform.

### Keywords

Mixing ventilation; Stratified air ventilation; Air curtain ventilation; Air distribution; Thermal comfort.

### 1. Introduction

Subway system represents the major transportation mode in most metropolitan areas worldwide, due to its unique characteristics: convenience, safety, efficiency, high speed, large transport capacity and low emission system [1]. Recently, a growing number of researchers [2][3][4][5] pay close attention to the subway-surrounding environment. However, the attainment of a comfortable indoor environment is not an easy task [2]. Air velocity and temperature in subway station impact directly on the passenger comfort and vertical temperature gradient presents a significant variation. Additionally, ventilation systems are widely used in underground subway stations to reduce various pollutants concentration [3]. Therefore, the design of a reasonable ventilation system is critical to obtain a comfortable environment in the subway station [4].

Due to the development of subway system during the last century, many studies investigated intensively the subway-surrounding environment. Thus, remarkable problems have arisen which attracted researchers consideration. Subway station is a crowded area including underground architecture, hence air distribution is difficult to predict. Furthermore, important factors affect air distribution, such as outdoor air pressure and air leakage through screen door. In addition, air quality and thermal comfort environment proved to be poor in occupied region when air distribution is not provided in an appropriate way. Ken Misawa et al. [5] demonstrated that local thermal environment on the platform could not meet passenger requirements. In addition, air quality is influenced by a series of factors, such as the ventilation system, station depth and design [6]. Therefore, each station specific conditions should be taken into consideration. Total suspended particulate (TSP) samples have been collected at six stations in Buenos Aires underground system and experimental results indicated that the TSP levels in stations and outdoor environment are poorly correlated [7]. T. Moreno [8] investigated air quality in Barcelona subway station and demonstrated that varies in each station. Furthermore, he suggested that platforms with large space provide a relatively good environment.

Three types of ventilation are widely used in subway platform: a) mixing, b) stratified air and c) air curtain. Different ventilation systems have their own advantages and disadvantages during application. To investigate air distribution under different ventilation systems on the platform, CFD simulations were performed to assess air distribution and thermal environment through a simplified platform model. Velocity, temperature, age of air and RWI in mixing ventilation, stratified air ventilation and air curtain ventilation were examined, compared and optimized to obtain an improved environment for passengers.

## 2. Physical And Numerical Modeling

In order to acquire a healthy and comfortable environment on the platform, three types of air-conditioning supply schemes were compared on the platform: a) mixing ventilation (scheme 1), b) stratified air ventilation (scheme 2) and c) air curtain ventilation (scheme 3). These three kinds of air supply diagrammatic sketches are illustrated in Figs. 1–3. Supply air temperature was set at 18 °C and the air-conditioning control temperature on platform was settled at 29 °C in summer. These three schemes approximately include an identical supply of airflow rate. Air velocity of three schemes were 1.39 m/s (scheme 1), 3 m/s (scheme 2) and 2.68 m/s (scheme 3), respectively. Under Fig. 1 (scheme 1), six groups of diffusers were installed at the ceiling to provide fresh air. The size of each diffuser was 0.4 m × 0.4 m and the distance between the two diffusers was about 3.5 m in each group. All six groups were positioned in a line parallel to the screen door. In Fig. 2 (scheme 2), 9 stratified air-conditioners with the height of 2.6 m were arranged near the pillars, with 8 spherical nozzles fixed on each of them. The cooling air was provided through the spherical nozzles to the occupied region. As Fig. 3 illustrates, 9 annular slots surrounded the pillars at the top of platform and the internal and external diameter equaled 0.85 m and 0.95 m, respectively.

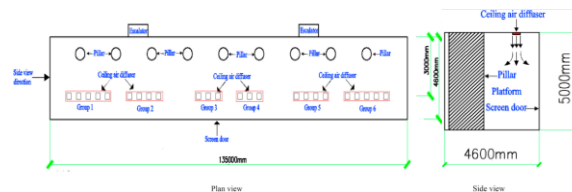


Fig. 1. Supply routine of scheme 1.

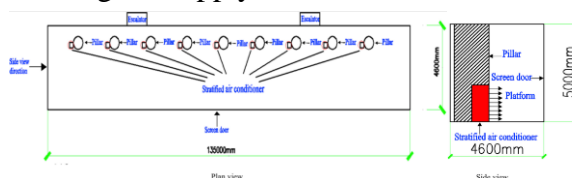


Fig. 2. Supply routine of scheme 2.

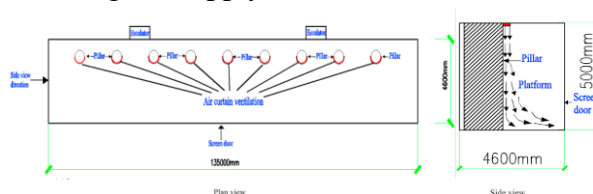


Fig. 3. Supply routine of scheme 3.

The air on the platform was assumed incompressible and the effects of density variation, which caused the buoyancy force, were taken into consideration by adopting Boussinesq approximation. Hence buoyancy was considered during the calculating procedure and the density was adopted as a variable only in the volume-force term in the momentum equation. During simulation, the velocity of airflow was low enough to neglect dispersion heat caused by viscosity force. It is assumed that high Reynolds number was acquired and the viscosity in all direction has the same properties.

The geometry used in the computations was identical to that used in the side platform. An automatic, unstructured hybrid element mesh generator was employed, which permitted an accurate representation of the boundaries. Grid refinement occurred around the inlet regions to provide an

accurate result since this region plays a significant role during the simulation procedure. There are three basic numerical grids with different quantities for each type of air supply scheme respectively. Mesh independency was examined for these kinds of grids, which aimed in finding an appropriate grid considering both accuracy and simulation time. The results of mesh-independency examination are presented in Fig. 4.

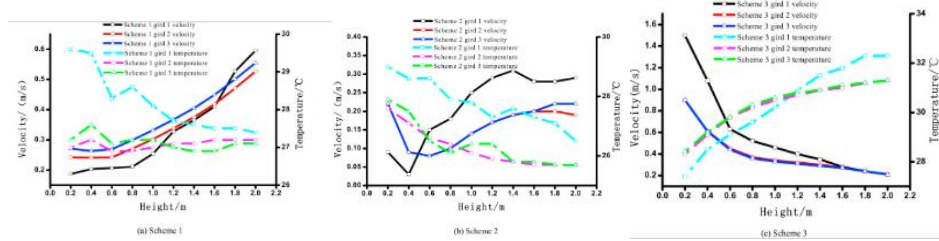


Fig. 4. Validation of mesh independence.

The numerical model, which based on the actual platform, was validated compared to results in the literature [4]. Fig. 5 illustrates the temperature profile comparison between predicted result and measured data, while a fair agreement is observed. For each of the ten points, the average temperature error between predicted and measured data was less than 1 °C. The values of predicted temperature were slightly higher compared to the measured data. By considering the accuracy of the measurements, values acquired by simulation prove the efficient and accurate performance of CFD model.

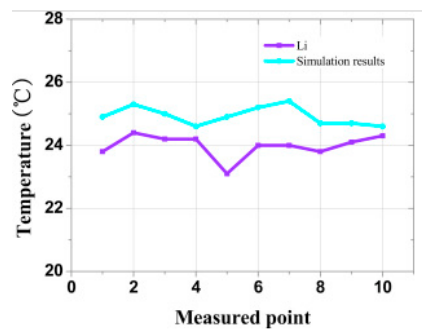


Fig. 5. Temperature profiles comparison between predicted result and measured data in the literature [4].

### 3. Results And Discussion

Fig. 6 illustrates the dimensionless velocity decay for scheme 1. Air velocity decreases by increasing of the dimensionless distance due to entrainment between fresh and indoor air. A previous study [9] demonstrates an analytical solution of vertical non-isothermal jet and simulation data match efficiently with Chen's analytical solution. In the range of 3.75–8.75, the decay of velocity in the simulation was slightly slower than the analytical solution given by Ref.[9] since airflow in one group impact on each other to form a large jet which causes less dissipation to maintain the velocity in the core. However, when dimensionless distance was at the range of 8.75–11.25, the velocity value presented a rapid decline due to the influence of ground, which constitutes a benefit for the passenger comfort.

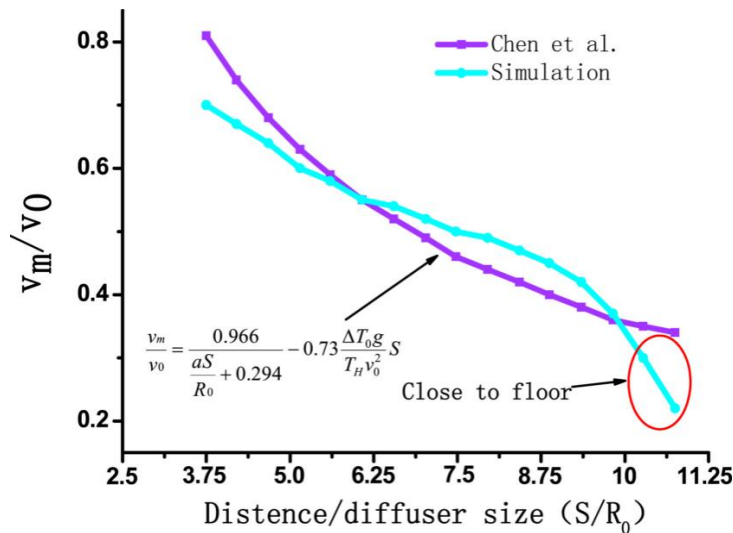


Fig. 6. Dimensionless velocity in scheme 1. Note:  $v_m$  and  $v_0$  represent the local maximum velocity and supply air velocity respectively.  $S$ ,  $a$ ,  $R_0$ ,  $g$  and  $T_H$  are the distance of jet, turbulence coefficient, radius, temperature difference between supply and room air, gravity and room air absolute temperature.

The dimensionless velocity decay for scheme 2 is illustrated in Fig. 7. Horizontal axis represents the dimensionless horizontal distance from the stratified air supply nozzle while vertical axis serves as dimensionless air velocity. The simulation results close to the nozzle were lower than the equation given by Ref. [10]. Nevertheless, the decay of velocity in predicted results was slower than analytical solution since the airflow from 8 nozzle converge together to prevent deceleration. This indicates that velocity retention was relatively satisfactory. When the dimensionless distance from nozzle equaled 10, the same velocity was obtained between simulation and analytical solution.

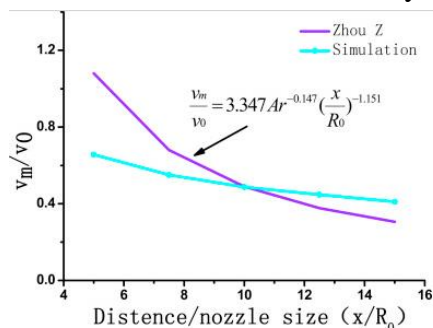


Fig. 7. Dimensionless velocity in scheme 2. Note:  $v_m$  and  $v_0$  represent the local maximum velocity and supply air velocity respectively.  $Ar$  is Archimedes number.  $R_0$  and  $x$  represent the radius and the distance of jet in horizontal direction.

For scheme 3, Fig. 8 illustrates the dimensionless velocity decay in wall jet region. The simulation result was compared with past studies as it concerns air curtain ventilation [11][12]. Although most of the simulated data were located between two equations, dimensionless velocity in this study declines more rapidly compared to that in the analytical solution at the range of 18–20, since airflow is close to the ground surface. Rapid decay of air velocity corresponds to relatively low air velocity in the occupied zone, which could provide a comfort region for passengers. In addition, when dimensionless distance was at a range of 13–18, the decay trend of velocity in predicted result was similar with the formula given in Refs.[13][14]. Therefore, the simulation result presented a satisfying agreement to the previous research.

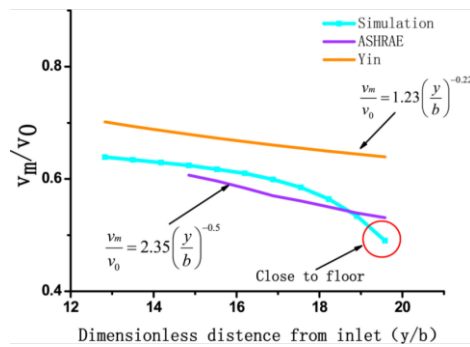


Fig. 8. Dimensionless velocity in scheme 3. Note:  $v_m$ ,  $v_0$ ,  $y$  and  $b$  represent the local maximum velocity, supply air velocity, distance of jet in vertical direction and the width of slot respectively.

Air velocity distribution at the height of 1.5 m was analyzed by including three schemes (Fig. 9). According to Fig. 9(a) (scheme 1), velocity values in the occupied region were less than 0.3 m/s excluding the region around air supply axis. This indicates that velocity in most of the occupied zone was acceptable for passengers [11] and uniformity of velocity on the platform was efficient for scheme 1. By observing scheme 2 (Fig. 9(b)), it is demonstrated that although velocity was low enough in the majority of the region, the highest velocity exceeds 1 m/s and was located near the stratified air supply equipment. The explanation for this could be the fact that fresh air was directly supplied to the occupied region at a high velocity since each air supply device corresponds to a large area of the platform. Furthermore, velocity was higher than 0.5 m/s around the screen door due to low deceleration of supply air. Fig. 9(c) represents the calculation result for scheme 3. The highest velocity was obtained close to the pillar area, since fresh air moved downwards to the ground area along them to maintain momentum and reduce air mixing. In wall jet region, velocity could achieve a value greater than 0.8 m/s, which contributes to decreased comfort of occupants. However, these does not represent the regions including high density of occupants, hence a few passengers would feel uncomfortable. At the center of two pillars, velocity was slightly higher than that in adjacent zone, which can be attributed to encounter of two streams supplied from two contiguous pillars. In addition, velocity in most of the regions was less than 0.3 m/s and uniform velocity distribution in the occupied region was acquired, which results in a comfortable environment for occupants.

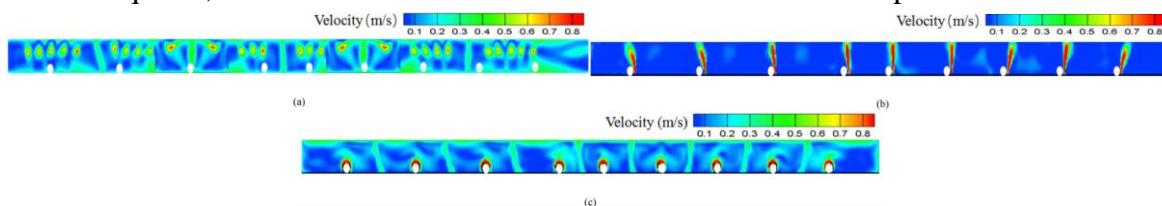


Fig. 9. Velocity distribution at height of 1.5 m in three schemes. (a) Velocity distribution in scheme 1 (b) Velocity distribution in scheme 2 (c) Velocity distribution in scheme 3.

According to the numerical calculation, air temperature distribution of 1.5 m height in three cases is illustrated in Fig. 10. Two regions including a temperature higher than 32 °C are presented in scheme 1 (Fig. 10(a)) which can be ascribed to less low temperature air supply. It is obvious to find that occupants would feel slight warm sensation under this condition. Temperature at both of the platform edges was relatively lower than adjacent regions since more diffusers were installed at this area compared to the rest place, offering a large quantity of fresh, low temperature air, mixing with indoor higher temperature air. It is distinct that the higher amount of fresh air is supplied, the lower temperature is obtained. According to Fig. 10(b), the result from numerical calculation presents that air temperature was between 27 °C and 30 °C at the center of platform, which corresponds to the region of the high density of air supply equipment, whereas air temperature was slightly higher at both of platform edges. By temperature drop exceedingly even below 22 °C near the air supply devices, a cold sensation could occur to passengers. This could occur since fresh air was directly sent to occupied region without mixing with higher temperature indoor air. Fig. 10(c) illustrates the air temperature distribution of scheme 3. By comparing Fig. 10(a), (b) and (c), it can be seen that the

efficient uniformity of air temperature distribution at height of 1.5 m above the ground can be achieved by adopting air curtain ventilation scheme. The temperature in most of the occupied areas falls within the range of 27 °C–30 °C, which provided a relative comfort region for passengers. Furthermore, air temperature was slightly lower at the intermediary region than other platform areas due to the large quantity of fresh air.

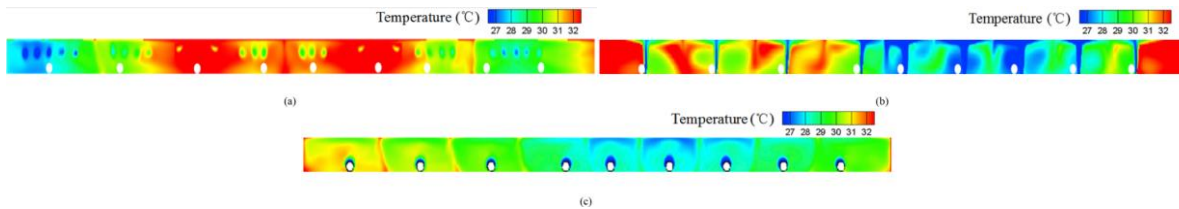


Fig. 10. Temperature distribution at height of 1.5 m in three schemes. (a) Temperature distribution in scheme 1 (b) Temperature distribution in scheme 2 (c) Temperature distribution in scheme 3.

The age of air on the platform in three schemes is presented in Fig. 11(a), (b) and (c) respectively. Results reveal that the age of air distributions in occupied region have remarkably changed by choosing different air supply schemes and keeping the cooling loads unchanged. According to Fig. 11(a) (scheme 1), despite the larger density of diffusers at both of platform edges, indoor air remained longer in these regions (more than 320 s), indicating a bad air quality for the passengers. Nevertheless, in some areas the corresponding time was less than 60 s, which can not only be attributed to high density of diffusers, but also efficient air distribution which ensured aged air vent out of platform in appropriate time. At both platform edges, the results in scheme 2 (Fig. 11(b)) were similar to those in scheme 1. Thus, the highest value of time was obtained since air presents a tendency to keep stationary or form vortices at the corners. Under the influence of fresh air, age of air was remarkably short around the stratified air supply devices. The numerical calculation results of scheme 3 are presented in Fig. 11(c). Age of air was shorter near the pillars compared to that close to screen door. An explanation to this phenomenon could be the fact that fresh air, which was supplied to the floor, requires a long time to pervade every corner of the platform due to low air velocity near the ground.

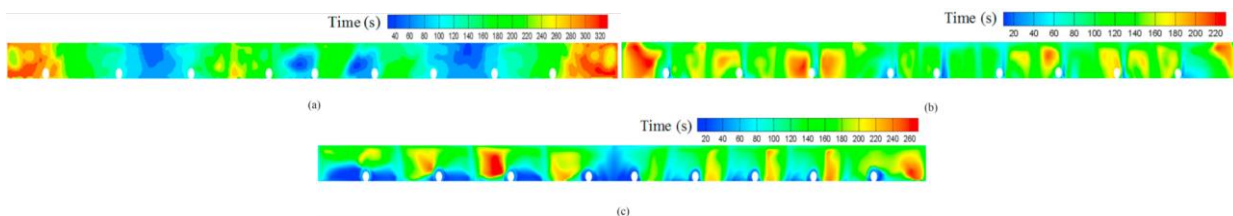


Fig. 11. Age of air at height of 1.5 m in three schemes. (a) Age of air distribution in scheme 1 (b) Age of air distribution in scheme 2 (c) Age of air distribution in scheme 3.

Fig. 12 illustrates the descriptive statistics of calculated RWI values on platform for the three schemes. The values of RWI were 0.305, 0.259 and 0.261, respectively. It can be concluded that thermal environment was relatively warm on the platform for the three schemes and the ideal thermal comfort has not been achieved. This comes to an agreement with Ampofo's [15] research which result demonstrated that the thermal comfort condition was slightly warm. However, the situation in scheme 2 and 3 was slightly improved compared to scheme 1, thus passengers could feel warmer with the air supply system of scheme 1, compared with other two schemes. Although it could provide a warm environment on the platform, passengers would leave the area as soon as possible, which would be propitious to management.

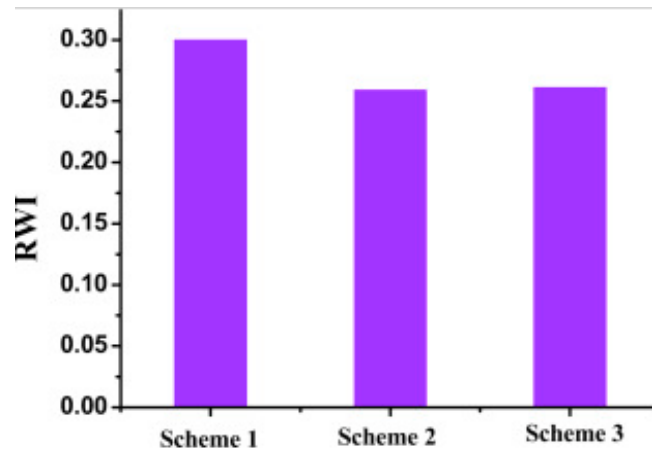


Fig. 12. RWI in occupied region for three schemes.

The values of dimensionless velocity with different supply air velocities in the range of 0.1 m–2 m are illustrated in Fig. 13. For these four cases, the decay of velocity was rapid at the dimensionless height range of 0.9–1 (area where passengers approach to the air supply devices), which was similar to the findings of Yin et al. [16].

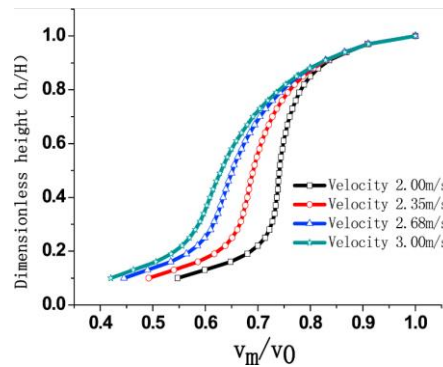


Fig. 13. Dimensionless velocity with different air supply velocity. Note:  $h$ ,  $H$ ,  $v_m$  and  $v_0$  represent the height of a certain point, the height of room, the local maximum velocity and supply air velocity respectively.

Fig. 14 illustrates the jet thickness in vertical direction, which could be a parameter to access the mixing degree of fresh air and indoor air. The thickness in the height range of 3 m–4.5 m in the four cases was almost identical, which corresponds to less than 0.4 m. However, the thickness was increased by accelerating air supply velocity when the height was in the range of 1 m–2.5 m. Thus, this indicates that fresh air in higher air supply velocity mixes with more indoor air in the vertical attached region. High air supply velocity case not only improved thermal comfort in occupied region by mixing indoor air, but also accelerated decay of velocity to meet the requirement. Simulation results demonstrate that although the thickness in this paper were slightly larger than the result achieved by Beltaos et al. [13], the tendencies of thickness increment were similar. In addition, the maximum difference of thickness between predicted results and Beltaos et al. work was less than 0.1 m. Due to the influence of floor, the thickness in four cases rapidly increased in the height of 0.5 m, which provided a relatively lower velocity in occupied zone for passengers.

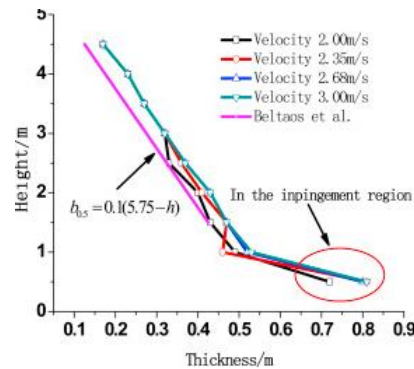


Fig. 14. Vertical jet thickness with different air supply velocity. Note:  $h$  and  $b_{0.5}$  represent the height of a certain point, the horizontal distance from the boundary to the point of half of the maximum velocity respectively.

Fig. 15 illustrates vertical velocity and temperature distribution at the height range of 0.1 m–2 m, which is located at the center of the platform, between screen doors and pillars. According to Fig. 15(a), by increasing height, the values of velocity increase in the range of 0.1 m–0.2 m and rapidly diminish when arrived at 0.2 m, whereas velocity distributions were almost stable in the height range of 1 m–2 m. Air temperature distributions in vertical direction were similar in four cases while the differences were particularly evident in the range of 0.1 m–0.2 m (Fig. 15(b)).

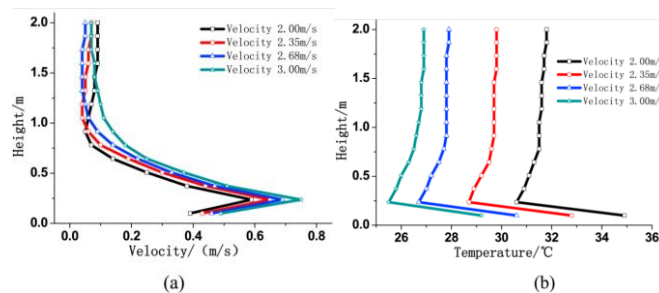


Fig. 15. Velocity and temperature distribution in vertical direction. (a) Vertical velocity distribution (b) Vertical temperature distribution.

#### 4. Conclusion

This paper presents a study of subway station platform that includes simulating air distribution and occupants' thermal comfort. The key conclusions are summarized below:

1. Three ventilation schemes (mixing ventilation, stratified air ventilation and air curtain ventilation) were compared by considering air velocity, air temperature, age of air and RWI. The uniformities of velocity and temperature distribution were satisfactory when air curtain ventilation was adopted. The mean age of air was 131s while the value of RWI exceeds 0.25. Although thermal condition was slightly warm on the platform, air curtain ventilation provides a healthy and comfortable environment compared with mixing ventilation and stratified air ventilation.

2. Under air curtain ventilation scheme, four cases presented the same tendency that rapid dimensionless velocity deceleration occurred around inlet and ground while the maintenance of dimensionless velocity was relative improved in the middle range. Decay of velocity was rapid in the dimensionless height range of 0.9–1. When the dimensionless height was at the range of 0.2–0.8, dimensionless velocity falls in the range of 0.7–0.8 in case 1, whereas it equaled approximately 0.6 in case 4, indicating that case 1 (2 m/s) represents the optimum condition to maintain velocity. Furthermore, case 4 (3 m/s) presented a fast deceleration in each of the four cases. Reduction of dimensionless velocity accelerates in all four cases when dimensionless height was between 0.1 and 0.2.

3. Air temperature and velocity distribution in vertical direction were almost stable when the height exceeded 1 m. The highest values of velocity were achieved at 0.2 m in four cases where the lowest



temperatures were obtained. Although the retention of dimensionless velocity in vertical direction improves by decreasing of air supply velocity, temperature was higher in the occupied region when the case with low velocity was applied. By considering all the factors, velocity and temperature distributions proved to be more appropriate when case 3 (2.68 m/s) is adopted.

4. When the air curtain ventilation scheme was designed, although the difference of air supply velocity on platform affects temperature distribution evidently in the occupied region, it has an insignificant influence on velocity distribution.

### Acknowledgements

This work is supported by the National Natural Science Foundation of China(No. 11602066) and the National Science Foundation of Heilongjiang Province of China (QC2015058 and 42400621-1-15047), the Fundamental Research Funds for the Central Universities.

### References

- [1] V. Martins, T. Moreno, L. Mendes, et al. Factors controlling air quality in different European subway systems *Environ. Res.*, 146 (2015), pp. 35-46
- [2] G. Ye, C. Yang, Y. Chen, Y. Li A new approach for measuring predicted mean vote (PMV) and standard effective temperature (SET\*) *Build. Environ.*, 38 (1) (2003), pp. 33-44
- [3] D.U. Park, K.C. Ha Characteristics of PM<sub>2.5</sub> and CO monitored in interiors and platforms of subway train in Seoul, Korea *Environ. Int.*, 34 (5) (2008), p. 629
- [4] J. Li Subway Station Air-conditioning Load Calculation Method Research Based on Field Measurement [D] Tsinghua University (2009)
- [5] K. Misawa, J. Nakano, S.I. Tanabe Field survey of thermal environment and occupancy condition of passengers in railway station *Cytopathology*, 27 (4) (2007), pp. 297-299
- [6] X. Querol, T. Moreno, A. Karanasiou, et al. Variability of levels and composition of PM<sub>10</sub> and PM<sub>2.5</sub> in the Barcelona metro system *Atmos. Chem. Phys.*, 12 (11) (2012), pp. 253-261
- [7] L.G. Murruni, V. Solanes, M. Debray, et al. Concentrations and elemental composition of particulate matter in the Buenos Aires underground system *Atmos. Environ.*, 43 (30) (2009), pp. 4577-4583
- [8] T. Moreno, N. Pérez, C. Reche, et al. Subway platform air quality: assessing the influences of tunnel ventilation, train piston effect and station design *Atmos. Environ.*, 92 (2014), pp. 461-468
- [9] S.L. Chen, M.Q. Xu, Z.Y. Chen Calculation about vertical different temperature jet axis velocity *J. Ningxia Inst. Technol.* (2) (1996), pp. 12-15
- [10] Z. Zhou Study of the applicability of jet theory for large space air conditioning *Heat. Vent. Air Cond.*, 40 (2) (2010), pp. 123-127
- [11] ASHRAE 1993 ASHRAE Handbook: Fundamental [M] American Society of Heating, Refrigeration and Air-Conditioning Engineers, Inc., Atlanta, USA (1993)
- [12] H.G. Yin, A.G. Li Study on airflow characteristics of attached air curtain ventilation model *J. Xi'an Univ. Archit. Technol.*, 47 (6) (2015), pp. 879-884
- [13] S. Beltaos, N. Rajaratnam Plane turbulent impinging jets *J. Hydraulic Res.*, 11 (1) (1973), pp. 29-59
- [14] H.J. Chen, B. Moshfegh, M. Cehlin Numerical investigation of the flow behavior of an isothermal impinging jet in a room *Build. Environ.*, 49 (3) (2012), pp. 154-166
- [15] F. Ampofo, G. Maidment, J. Missenden Underground railway environment in the UK Part 1: review of thermal comfort *Appl. Therm. Eng.*, 24 (5) (2004), pp. 611-631
- [16] H.G. Yin, A.G. Li Airflow characteristics by air curtain jets in full-scale room *J. Central South Univ.*, 19 (3) (2012), pp. 675-681